NANO LETTERS

2007
Vol. 7, No. 2
351−356

Composite Organic–Inorganic Nanoparticles as Raman Labels for Tissue Analysis

Lei Sun,[†,‡] Kung-Bin Sung,[†,‡] Claire Dentinger,[†] Barry Lutz,[†] Lienchi Nguyen,[†] Jingwu Zhang,[†] Haoyu Qin,[†] Mineo Yamakawa,[†] Manqiu Cao,[†] Yu Lu,[†] AJ Chmura,[†] Jing Zhu,[†] Xing Su,[†] Andrew A. Berlin,[†] Selena Chan,*[,†] and Beatrice Knudsen*[,§]

Biomedical/Life Sciences, Digital Health Group, Intel Corporation, SC3-41, 2200 Mission College Boulevard, Santa Clara, California 95054, and Division of Public Health Sciences, Fred Hutchinson Cancer Research Center, M5-A864, 1212 Aloha Street, Seattle, Washington 98054

Received October 19, 2006; Revised Manuscript Received December 22, 2006

ABSTRACT

Composite organic–inorganic nanoparticles (COINs) are novel optical labels for detection of biomolecules. We have previously developed methods to encapsulate COINs and to functionalize them with antibodies. Here we report the first steps toward application of COINs to the detection of proteins in human tissues. Two analytes, PSA and CK18, are detected simultaneously using two different COINs in a direct binding assay, and two different COINs are shown to simultaneously label PSA in tissue samples.

Tissue-based analysis of protein expression provides crucial diagnostic and prognostic information. Currently, immunohistochemistry (IHC) is the most widely used method to measure protein expression in tissues. The detection of analytes in tissue sections can be accomplished through antigen−antibody interactions using antibodies labeled with fluorescent dyes, enzymes, radioactive compounds, or colloidal gold. Multiplex tissue analysis, in which two or more analytes are detected simultaneously, is a powerful approach to study coexpression and spatial distribution of protein expression, while consuming fewer tissue samples. Currently, multiplex tissue analysis is performed by sequential staining of a tissue sample using either enzyme- or dye-labeled antibodies.[1,2] However, this approach is limited by several factors: i, overlap of fluorescence dye signals due to their large emission peak width (>50 nm); ii, lengthy assay protocols; and iii, specificity of the secondary antibody detection reagents. Recent advances in nanoparticle technology have led to the development of quantum dots (QDs), which are semiconductor nanocrystals with size-dependent fluorescence emission. Multiplex tissue analysis using quantum dots[3−5] has advantages over traditional dyes due to improved photostability, higher intensity, and narrower emission peaks (∼30 nm in peak width).

Raman-based nanoparticles are another class of emerging labels.[6−13] Typical Raman scattering intensity is very low compared to fluorescence, but the Raman scattering efficiency can be greatly enhanced by adsorbing Raman-active molecules onto the surface of metal nanoparticles or roughened metal substrates.[14,15] Surface-enhanced Raman Scattering (SERS) provides 10^6-10^{14}-fold of enhancement in Raman signal intensity, which is sufficient for single-molecule detection.[16−18] Compared with traditional fluorescence labels, Raman nanoparticles have much narrower emission peaks (<2 nm) and offer the potential to develop an increased number of unique optical "signatures" by varying the structures of the embedded Raman active molecules. These characteristics make them ideally suited for multiplexing. Raman nanoparticles also have other advantages, such as (i) the lack of photobleaching, (ii) single laser excitation for detection of multiple labels, and (iii) easy distinction from the background autofluorescence signal of biological samples.

Several types of Raman nanoparticles have been developed in recent years, two of which will be further discussed. The first consists of gold nanoparticles that are coated with Raman active molecules and stabilized through silica coating.[6−10] Another type is composite organic−inorganic nanoparticle (COIN), which is a nanocluster formed by

* Corresponding authors. E-mail: bknudsen@fhcrc.org; selena.chan@intel.com.
† Intel Corporation.
‡ Both authors contributed equally to this work.
§ Fred Hutchinson Cancer Research Center.

10.1021/nl062453t CCC: $37.00
Published on Web 01/17/2007

aggregating silver nanoparticles in the presence of Raman-active molecules.[11] Exploiting the fact that the SERS effect is stronger in nanoparticle aggregates,[12] COIN provides higher Raman intensity than gold-based Raman nanoparticles. Additionally, COIN's unique chemistry enables use of a broader range of Raman-active molecules. Specifically, COIN is not limited to molecules that have specific metal-binding functional groups such as isothiocyanide and thiol, which are required for gold Raman nanoparticles. In a previous report, we demonstrated the use of COIN for quantitative and sensitive detection of proteins in a sandwich assay format.[11]

In this paper, we present methods for stabilizing and functionalizing COINs and applying them to tissue-based analyses. We demonstrate the use of COIN−antibody conjugates in a multiplex direct binding protein assay, and we extend this assay to a tissue-imaging application. The high Raman intensity and multiplex potential of COINs demonstrate their ability to simultaneously "color" multiple proteins in a single tissue sample without enzymatic amplification.

Encapsulation is a crucial step before a nanoparticle label can be applied in a bioassay. It stabilizes the nanoparticle by preventing aggregation and disintegration and introduces surface functional groups for biomolecule attachment. To encapsulate COINs, bovine serum albumin (BSA) and glutaraldehyde are introduced to the colloidal COIN solution to form a cross-linked organic encapsulation layer around the COIN. The extra aldehyde functional groups on the COIN surface are then removed by treatment with glycine or sodium borohydride. Since most of the surface amino groups on the protein layer are removed in this process, the encapsulated COIN carries a net negative charge from the carboxylic acid groups, as characterized by zeta-potential measurements (see Supporting Information). The size of encapsulated COIN is typically 60−100 nm, and the thickness of the encapsulation layer is about 10 nm according to photon correlation spectroscopy measurements. COINs' Raman spectra do not change after encapsulation, since the signal from the Raman label embedded in the COIN is enhanced much more than the signal from BSA molecules surrounding the COIN. The size and Raman intensity of the BSA encapsulated COIN are stable in high-salt bioassay buffers such as PBS, and they can be stored for more than 6 months at 4 °C (see Supporting Information). Compared to other types of nanoparticle encapsulation methods, such as silica coating[8,9] and polymer coating,[19] the BSA encapsulation method is simpler and more efficient.

The functionalization of an encapsulated COIN with antibodies requires the activation of the carboxylic acid groups on the BSA molecule by *N*-(3-(dimethylamino)-propyl)-*N*′-ethylcarbodiimide (EDC). Excess EDC is removed by centrifugation, and the resulting *O*-acylisourea intermediates are reacted with amino groups from the antibodies to form amide bonds between the encapsulation layer and the antibodies. We evaluated a number of reaction conditions and found that reaction in 10 mM of sodium borate buffer gives the highest yield (∼50%) as measured

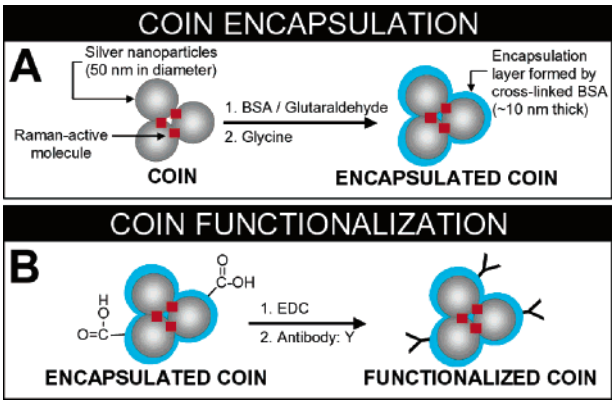

Figure 1. COIN encapsulation and functionalization method. (A) Schematic illustration of COIN encapsulation procedure. Bovine serum albumin (BSA) is coated to the COIN surface and cross-linked by glutaraldehyde. The extra aldehyde functional groups on the COIN surface are removed by glycine and sodium borohydride treatment. (B) Schematic illustration of COIN functionalization procedure. Carboxylic acid groups on the surface of the BSA encapsulation layer are activated by EDC and reacted with amines groups in the antibody.

by UV absorption (see Supporting Information). The quality of the COIN−antibody conjugate is confirmed by a protein sandwich binding assay as described in our previous paper.[11] A schematic illustration of the COIN encapsulation and functionalization method is shown in Figure 1.

In this paper, we focus on applying the encapsulated and functionalized COIN as a distinct optical label for tissue protein expression. Formalin-fixed tissue is a challenging sample due to its molecular heterogeneity and the inherent tissue autofluorescence. Protein expression varies within different regions of the tissue surface, and the concentrations of the proteins within the tissue cannot be determined. Therefore we developed a direct binding method to test the COIN in a simple and controllable assay that mimics the tissue analysis. In this assay, the protein analyte is directly immobilized on a solid surface and detected by a COIN-conjugated antibody. The binding of protein analytes to the aldehyde surface eliminates certain epitopes within proteins or renders them inaccessible to antibody detection reagents, thereby mimicking in part the loss of antigenicity as it occurs during protein cross-linking and slide preparations with human tissues. In the direct protein binding assay, we immobilize prostate specific antigen (PSA), a protein expressed in prostate tissue, at increasing amounts in isolated wells on aldehyde-coated glass slides. Immobilized PSA protein is probed with COIN−antibody conjugates (Figure 2A). The specific COINs used in this experiment are constructed with the Raman-active molecule Basic Fushin, encapsulated, and functionalized by PSA antibodies (BFU−AbPSA). COIN Raman spectra are acquired using a home-built Raman spectroscopy system with 514 nm laser excitation and 0.1 s exposure time. The assay is run in parallel wells under the same conditions to reduce variations that are not relevant to COIN performance on tissue (e.g., antigen incubation time), and data are averaged from a raster of 400 points within each well to account for possible variation of antigen distribution on the plate. The averaged spectra from

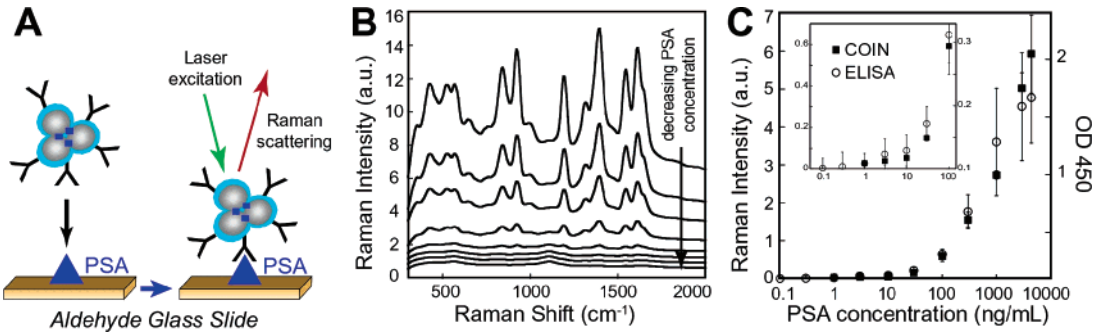

Figure 2. COIN−antibody conjugates in the direct protein binding assay. (A) Schematic representation of a direct binding assay. (B) Representative Raman spectra from a direct binding experiment in which different concentrations of PSA are detected by COIN functionalized with anti-PSA antibody (BFU−AbPSA). Solution PSA concentrations from top to bottom are 3000, 1000, 300, 100, 30, 10, 3, and 1 ng/mL, respectively. Each spectrum is generated from an average of 400 spots in a well that is coated with a different amount of PSA. (C) Comparison between COIN and ELISA in a direct binding assay. Raman signal intensities (squares) of the 1610 cm^{-1} peak of BFU−AbPSA and adsorption at 450 nm from ELISA (circles) are plotted as a function of PSA concentration. The insert expands the scale so that the limit of detection for COIN and ELISA assays can be better visualized. Error bars represent the standard deviation between three or four replicate wells.

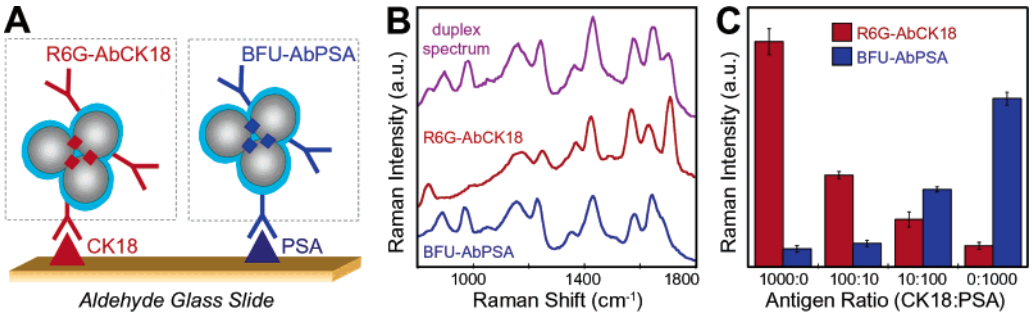

Figure 3. Multiplex direct protein binding assay with COIN. (A) Schematic representation of a duplex direct binding assay detecting PSA and CK18 analytes. PSA and CK18 proteins are immobilized together in the same well. (B) The purple line (upper) is the Raman spectrum from a duplex direct binding experiment in a well coated with both PSA and CK18 and detected by BFU−AbPSA and R6G−AbCK18 COIN−antibody conjugates. Blue (lower) and red (center) lines represent single spectra from BFU−AbPSA and R6G−AbCK18 measured in separate wells coated with only PSA or only CK18, respectively. (C) Signal intensities from a duplex direct binding experiment using different concentration ratios of CK18 and PSA immobilized proteins. The signal from each COIN is extracted from the duplex spectrum. Error bars represent the standard deviation of Raman signal from four replicate wells.

the PSA-coated wells are depicted in Figure 2B. The direct binding assay with COIN is validated by comparison with an ELISA direct binding assay conducted in parallel wells. Representative results for quantitative measurements of Raman intensities and ELISA absorption at various concentrations of PSA are shown in Figure 2C. For both COIN and ELISA assays, the lower limits of detection (LLD) for four to six repeat experiments are between 1 and 10 ng/mL PSA added in solution (inset in Figure 2C). The dynamic range of the PSA direct binding assay is 1−3000 ng/mL PSA added in solution for the COIN assay and 1−1000 ng/mL for the ELISA assay. The intra-assay variability, measured as the coefficient of variance between at least three replicate wells, is 16% for both the COIN and ELISA assays. It is important to note that the sensitivity reported here is different from the sensitivity measured from sandwich assays, as PSA protein directly bound to the solid substrate will have different immobilization efficiency and likely lower activity. Ultrasensitive detection of soluble PSA has been demonstrated by a variety of methods that take advantage of immobilized capture antibody to enrich PSA from serum samples and improve detection levels;[6,9,20,21] however these methods are not applicable in tissue analysis.[22] The results show that the COIN performance in a direct binding assay is comparable to a well-known, sensitive detection method, while the direct binding format provides a means of testing COIN on a surface that mimics the loss of antigenicity found in tissue samples.

As a first step to evaluate the multiplex potential of our technology, we tested 2 different COIN−antibody conjugates in a direct binding assay. Cytokeratin-18 (CK18), a protein expressed in benign and cancerous prostate epithelial cells, was chosen as the second protein analyte in this study. A Rhodamine 6G COIN (R6G-COIN) was conjugated to CK18 antibodies (R6G−AbCK18) and BFU-COIN was conjugated to PSA antibodies (BFU−AbPSA). Recombinant PSA and CK18 proteins were simultaneously immobilized on aldehyde-functionalized glass slides at different concentrations. The slides were then probed with a 1:1 mixture of R6G−AbCK18 and BFU−AbPSA conjugates as shown by the schematic in Figure 3A. Figure 3B shows the Raman spectra from different wells coated only with PSA, only with CK18, or both PSA and CK18. The spectrum obtained from a well coated with PSA and CK18 (purple) represents the combination of Raman signals obtained from each of the two COINs. To extract the Raman spectra of individual COINs, the

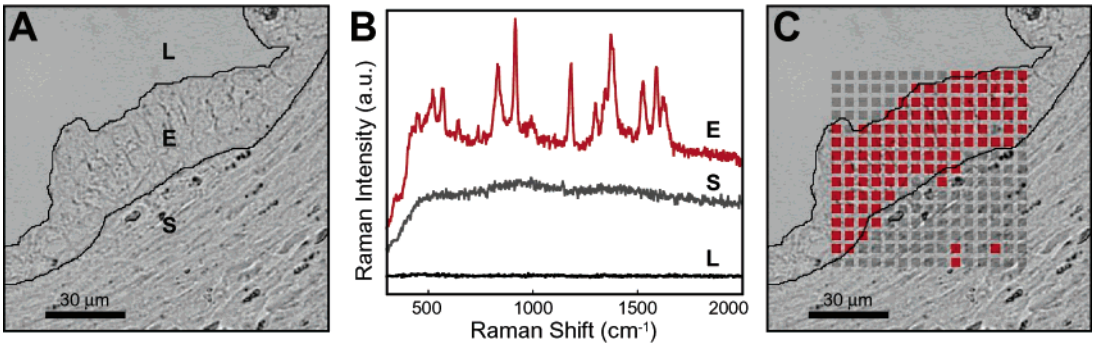

Figure 4. Spatial mapping of prostate-specific antigen (PSA) on tissue sections using COIN. (A) Brightfield image of a prostate gland showing three tissue compartments: the open lumen (L), epithelium (E), and stroma (S). (B) Representative spectra from the three regions of panel A from a tissue stained by BFU−AbPSA. Strong BFU−AbPSA signal is seen in the epithelium (E, red), where PSA is expressed at high levels. The stroma, which does not express PSA, shows a high level of tissue autofluorescence (S, gray), and the spectrum from the lumen is that of glass (L, black). Each spectrum is recorded from a single point using an acquisition time of 0.1 s; these spectra and their intensities are representative of spots in epithelium, stroma, and lumen recorded in this experiment. (C) PSA expression pattern in the tissue. Each square represents a single acquisition point in a raster pattern across the sample. Each point is classified as PSA-positive (red pixels) or PSA-negative (gray pixels) based on the intensity of the measured COIN signal using a single fixed threshold.

multiplex spectra were deconvoluted by ordinary least-squares (details in Supporting Information). The processed data from this duplex experiment using four different relative concentrations of PSA and CK18 is shown in Figure 3C. The Raman intensity for the R6G-AbCK18 (red) is proportional to the CK18 concentration and the Raman intensity from the BFU−AbPSA (blue) is proportional to the PSA concentration.

To demonstrate the feasibility of using COIN technology for tissue analysis, we applied the COIN conjugates to detect PSA in formalin-fixed, paraffin-embedded tissue samples from human prostate. While PSA is not a reliable marker for prostate cancer detection, the same functionalization and assay approach used here can create COIN probes to target other tissue proteins for which quality antibodies have been identified. Because of COIN's high signal intensity, the tissue binding assay can be conducted using a low concentration (~30 pM) of COIN−antibody conjugate without the need for secondary amplification, and the Raman data can be collected using a relatively low power laser (0.3 mW) and very short signal acquisition times (0.1 s). The single-step staining procedure is significantly shorter than traditional immunohistochemistry because steps such as incubation with secondary antibodies, enzymatic color development time, and endogenous biotin blocking steps are all eliminated. The low instrument power requirement and short collection time also represent an improvement over previously reported Raman analysis of tissue and cell samples.[10,13]

Figure 4A shows a brightfield image of a region of prostate tissue. Each prostate gland is lined by a layer of epithelial cells (E) surrounding an open lumen (L). Glands are embedded in supporting tissue, generally known as stroma (S). Figure 4B shows a representative spectrum from each region of tissue after staining with BFU−AbPSA. Within the lumen, only the low-level background spectrum from glass is present (black), while the stroma shows a high level of tissue autofluorescence, which is characterized by a broad emission (S, gray). This autofluorescence poses a major limitation for immunofluorescence detection because it is difficult to distinguish the background autofluorescence from the broad spectra of fluorescent dyes. While it is possible to mitigate the autofluorescence problem by using fluorescence labels excited in the red to near-infrared region, it drastically limits the number of fluorescent labels available for multiplexing. In contrast, the unique pattern of narrow peaks in the COIN spectrum distinguishes it from the shape of the autofluorescence spectrum and allows identification and quantification of the COIN signal even in tissue areas containing a high level of autofluorescence. In Figure 4B, the spectrum taken from a spot in the epithelium (E, red) shows the distinct signature of the BFU−AbPSA, and the sharp peaks of COIN stand out clearly above tissue autofluorescence signal. To quantify the COIN signal from tissue samples, we use the least-squares approach that we also applied in the direct binding assay (see Supporting Information). This method allows deconvolution of the COIN signal from autofluorescence and other background signals.

PSA is expressed throughout the epithelium in both healthy and cancerous prostate glands. Here, we use COIN−antibody conjugates to create a spatial map of PSA expression in prostate tissue, and we characterize the quality of COIN staining by comparing it to the expected PSA expression pattern. Spectra are collected throughout defined points in a raster scan, and after extraction of the COIN signal by the least-squares method, each spot on the tissue is classified as PSA-positive or PSA-negative based on a single fixed intensity threshold. Figure 4C shows an image in which the PSA expression pattern is reported by the COIN, where red pixels represent spots with signal intensities above the threshold and gray pixels indicate negative locations. A small number of PSA-positive spots are noted outside the epithelium, which is likely due to nonspecific binding of the PSA antibody or COIN. This background signal is typically small (<10% of positive signal), and we find that the antigen is saturable at high COIN concentration, which demonstrates specificity for this assay.[23] The antibody−COIN detects PSA with high sensitivity (i.e., nearly every point in the epithelium is classified as PSA-positive) and high specificity (i.e., nearly

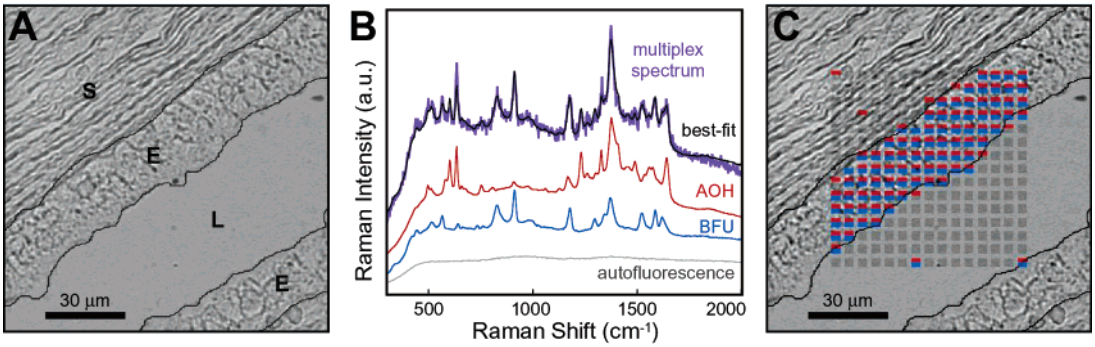

Figure 5. Simultaneous two-COIN staining for PSA antigen. (A) Brightfield tissue image showing stroma (S), epithelium (E), and lumen (L). (B) Spectral fitting in duplex COIN experiments on tissue. The upper set of spectra are the measured spectrum from a single point in the epithelium (purple) and the best-fit spectrum (black) found from least-squares regression using reference spectra. The major fitting components are the two conjugated COIN (red, AOH-AbPSA; blue, BFU-AbPSA) and the tissue autofluorescence (gray). For this experiment, the difference between the measured and best-fit spectra was less than 5% (average across the spectral range). The measured spectrum (purple) was acquired in 0.1 s. (C) PSA expression patterns reported by two COINs in a simultaneous duplex measurement. In each pixel, color represents PSA-positive classification based on BFU−AbPSA (blue) and AOH−AbPSA (red), and gray represents PSA-negative classification. Both COIN report PSA-positive expression for nearly every point in the epithelium (i.e., pixels with red and blue).

every point outside the epithelium is classified as PSA-negative). We have quantified the accuracy of staining for repeated measurements within different glands on multiple tissue samples, and we routinely find accuracies greater than 90% (i.e., percentage of correct classification for all points).

A central advantage of the Raman-based label is the distinct spectral signature, which is ideally suited for distinguishing individual COIN signatures in a complex spectral tracing. To illustrate the multiplex capabilities of COINs in tissue staining, BFU−COIN and AOH−COIN[24] are conjugated to anti-PSA antibodies, and both COIN−antibody conjugates are simultaneously applied to the tissue (Figure 5A). We reasoned that when antibodies bind to the same protein in the tissue sample, the potential risk of steric hindrance from the COINs is greater. Further, by choosing to target a single analyte, we set up the most difficult situation for deconvolution, in which the mixed signals from both COINs should be present at every spot. The major components of the spectrum determined from least-squares analysis (Figure 5B) are signals from BFU−AbPSA (blue), AOH−AbPSA (red), and tissue autofluorescence (gray). The best-fit spectrum is indicated in black, and the small error shown is typical of this kind of duplex experiment. The COIN is much smaller (60−100 nm) than the laser beam spot (0.8 μm), and unique peaks from each of the two COINs are easily visible in the raw spectrum captured from the epithelium (Figure 5B, purple spectrum), indicating the presence of both types of COIN at individual spots in the raster. The PSA expression pattern reported for each COIN is shown in Figure 5C, where red and blue indicate classification as PSA positive by AOH−AbPSA and BFU−AbPSA, respectively, and gray represents classification as PSA negative. Both COINs are detected in almost all spots, suggesting that steric hindrance of COINs does not represent a major problem. As with the single-COIN stain in Figure 4, high sensitivity and specificity are achieved for the combination of COINs.

The opportunity to stain a single biopsy with several distinct optical labels facilitates the simultaneous detection of multiple proteins in a small tissue sample and thereby increases the molecular information that can be obtained when amounts of tissue are a limiting factor. We have demonstrated that the signals from multiple COIN labels can be separated to generate maps of protein expression in tissue sections. In addition, the brightness of the COIN label and the narrow peak widths of the COIN signature effectively abolish the problem of tissue autofluorescence, which consists of a single broad peak. We are currently working to apply COIN to simultaneous detection of multiple antigens on tissues. The ability for quantitative analysis is limited by variation in the COIN signal intensity introduced during fabrication, and we are improving the homogeneity of the COIN preparation as a step toward quantitative detection.

Acknowledgment. The authors thank Kim Adolphson at the Fred Hutchinson Cancer Research Center for preparing the tissue samples and providing suggestions and Dr. Mark Roth at the Fred Hutchinson Cancer Research Center for inspiring discussions. The authors also sincerely thank the Intel Digital Health Group's Biomedical/Life Science research team for their continuous support.

Supporting Information Available: A list of materials and description of methods including COIN characterization and functionalization This material is available free of charge via the Internet at http://pubs.acs.org.

References

(1) Ellmark, P.; Belov, L.; Huang, P.; Lee, C. S.; Solomon, M. J.; Morgan, D. K.; Christopherson, R. I. *Proteomics* **2006**, *6*, 1791−802.
(2) Szeszel, M. K.; Crisman, C. L.; Crow, L.; McMullen, S.; Major, J. M.; Natarajan, L.; Saquib, A.; Feramisco, J. R.; Wasserman, L. M. *J. Histochem. Cytochem.* **2005**, *53*, 753−762.
(3) Alivisatos, A. P. *Nat. Biotechnol.* **2004**, *22*, 47−52.
(4) Seydack, M. *Biosens. Bioelectron.* **2005**, *20*, 2454−2469.
(5) Fu, A.; Gu, W.; Larabell, C.; Alivisatos, A. P. *Curr. Opin. Neurobiol.* **2005**, *5*, 568−75.
(6) Cao, Y.; Jin, R.; Mirkin, C. *Science* **2002**, *297*, 1536−1540.
(7) Mulvaney, S. P.; Musick, M. D.; Keating, C. D.; Natan, M. J. *Langmuir* **2003**, *19*, 4784−4790.
(8) Doering, W. E.; Nie, S. *Anal. Chem.* **2003**, *75*, 6171−6176.

(9) Grubisha, D. S.; Lipert, R. J.; Park, H. Y.; Driskell, J.; Porter, M. D. *Anal. Chem.* **2003**, *75*, 5936−5943.
(10) Schlucker, S.; Kustner, B.; Punge, A.; Bonfig, R.; Mar, A.; Strobel, P. *J. Raman Spectrosc.* **2006**, *37*, 719−721.
(11) Su, X.; Zhang, J.; Sun, L.; Koo, T.−W.; Chan, S.; Sundararajan, N.; Yamakawa, M.; Berlin, A. A. *Nano Lett.* **2005**, *5*, 49−54.
(12) Khan, I.; Cunningham, D.; Littleford, R. E.; Graham, D.; Smith, W. E.; McComb, D. W. *Anal. Chem.* **2006**, *78*, 224−230.
(13) Kim, J. H.; Kim, J. S.; Choi, H.; Lee, S. M.; Jun, B. H.; Yu, K. N.; Kuk, E.; Kim, Y. K.; Jeong, D. H.; Cho, M. H.; Lee, Y. S. *Anal. Chem.* **2006**, *19*, 6967−6973.
(14) Campion, A.; Kambhampati, P. *Chem. Soc. Rev.* **1998**, *27*, 241−250.
(15) Chan, S.; Kwon, S.; Koo, T.−W.; Lee, L. P.; Berlin, A. A. *Adv. Mater.* **2003**, *15*, 1595−1598.
(16) Nie, S.; Emory, S. R. *Science* **1997**, *275*, 1102−1106.
(17) Kneipp, K.; Kneipp, H.; Kartha, V. B.; Manoharan, R.; Deinum, G.; Itzkan, I.; Dasari, R. R.; Feld, M. S. *Phys. Rev. E* **1998**, *57*, R6281−R6284.
(18) Koo, T.-W.; Chan, S.; Sun, L; Su, X.; Zhang, J.; Berlin, A. A. *Appl. Spectrosc.* **2004**, *58*, 1401−1407.
(19) McCabe, A. F.; Eliasson, C.; Prasath, R. A.; Hernandez-Santana, A.; Stevenson, L.; Apple, I.; Cormack, P. A. G.; Graham, D.; Smith, W. E.; Corish, P.; Lipscomb, S. J.; Holland, E. R.; Prince, P. D. *Faraday Discuss.* **2006**, *132*, 303−308.
(20) Harma, H.; Soukka, T.; Lovgren, T. *Clin. Chem.* **2001**, *47*, 561−568.
(21) Zheng, G.; Patolsky, F.; Cui, Y.; Wang, W. U.; Lieber, C. M. *Nat. Biotechnol.* **2005**, *23*, 1294−1301.
(22) While sensitive detection of PSA from solution is not our goal, we note that by using COIN in a sandwich binding format, PSA detection sensitivity is improved by 2−3 logs (i.e., 10 pg/mL) compared to the direct binding format reported here. Detection limit of 1 pg/mL for solution PSA was reported[9] using another type of Raman nanoparticle label in sandwich assay with longer detection time. The lower sensitivity in direct binding assay is the result of low immobilization efficiency of PSA and loss of antigenicity after immobilization. Since our focus is on tissue-based analysis, we have not attempted to reduce detection limits for direct binding assay using COIN.
(23) We varied the COIN concentration from 0.125 to 1.0 mM and found saturation of the signal for concentrations approximately greater than 0.5 mM.
(24) AOH−COIN is fabricated with Raman active molecule Acridine Orange. BFU−COIN and AOH−COIN are selected for multiplex tissue analysis because they have similar signal to noise intensity ratio in tissue analysis.

NL062453T